LETTER REPORT

EVALUATION OF CRACKS ON THE JOSEPH M. FARLEY UNIT #1 MAIN STEAM ISOLATION VALVE (MSIV) SHAFT

Carl J. Czajkowski

Materials Technology Division
Department of Nuclear Energy
Brookhaven National Laboratory
Upton, New York 11973

AUGUST 1984

INTRODUCTION

In February 1984, during a refueling outage at the Joseph M. Farley Unit #1 Nuclear Power Station, linear indications were discovered on three of six main steam isolation valve (MSIV) shafts. The indications, which ranged in length from one to thirteen inches were found during cleanup of the shafts prior to reassembly of the valves. All indications were in the operator side packing gland area. Two of the shafts had only longitudinal indications, while the third shaft had both longitudinal and circumferential indications.

The three cracked shafts were all made of a 410 stainless steel with heat number HT 62687. The utility has planned to replace all three shafts with A564 GR 60 stainless steel as a preventative measure.

In order to more fully characterize the failure mode of these indications, the U. S. Nuclear Regulatory Commission (USNRC) Region II, Atlanta, Georgia, had one of the shafts (with only longitudinal indications) sent to Brookhaven National Laboratory (BNL) for a failure analysis. The analysis was to consist of:

a) Visual/Photography
b) Optical Microscopy, Chemical Analysis, and Hardness Testing
c) Scanning Electron Microscopy (SEM)/Energy Dispersive Spectroscopy (EDS)

This letter report is documentation of the failure analysis.

VISUAL/PHOTOGRAPHY

The MSIV shaft sent to BNL was #69C. The shaft "as received" was 77 inches long (195.6 cm) by 3.5 inches diameter (8.89 cm) and weighed approximately 400 lbs. The linear indications were located at the approximate halfway point on the shaft (Figure 1). The indications (cracks) encompassed a total length of approximately 6.6 inches (16.7 cm) axially along the shaft (Figure 2).

Seven discs were cut from the shaft (Figure 2) in the area of the cracks. All cuts were made dry in order to keep contamination to a minimum. The specimens cut were numbered 1-7. Specimens 2, 6 and 7 were used for SEM/EDS examination and specimens 4 and 5 were polished for optical metallographic examination. Specimen 1 had hardness measurements performed on it and then had half of the disc sectioned for chemical analysis.

After initial cutting, discs 2, 6 and 7 had counter notches cut in them (also cut dry), were soaked in liquid nitrogen, and then were broken open by applying a bending moment to them. One half of discs 2 and 7 were kept intact for SEM/EDS evaluation (with both halves of disc 6), while one half of each of the fracture faces were sent to photomicrography. Figures 3 and 4 are photographs of the fracture faces of disc 2 and 7, respectively. It is evident that both fractures had a thumbnail-like shape and were granular in appearance. Both surfaces were covered by a heavy oxide film which appeared black near the crack initiation areas and was lighter in appearance the greater the distance traversed from the initiation surface. This sort of appearance is typical of cracks which have been pre-existing for a good deal of time prior to propagation. Discussions with Messr. Troup and Crowley of USNRC, Region II, disclosed the fact that the shafts had been dye penetrant inspected prior to installation, which precluded the possibility of pre-existing quenching cracks in the material. On neither face was there any gross evidence of fatigue contribution (beach marks, etc.).

CHEMICAL ANALYSIS/HARDNESS TESTING/OPTICAL MICROSCOPY

As previously stated, one half of the first disc cut (specimen #1) was sent out for chemical analysis. The results of this analysis are shown in Table 1. The elemental analysis shows that the material in the shaft met the chemical requirements for an AISI 410 stainless steel.

A series of hardness traverses was made across the cross section of specimen #1. The hardness measurements were done both as Rockwell "C" scale and then again as microhardness measurements (Knoop). The results are shown in Table 2. The average of the ten microhardness measurements was 444 KN/500 gms,

which equates to R_C 43.4. The highest measurement was 459, which is R_C 44.5. The Rockwell C hardness tests had an average of R_C 41.25. Discussions with USNRC Region II regarding the shaft's heat treatment revealed that they had been quenched from 1775°F $\pm$ 25°F in either air or oil, and then tempered at 950°F to a hardness of Brinell 345-370 (R_C 37-39.8), which would be significantly lower than the actual recorded hardness readings.

Specimens 4 and 5 were ground, metallographically polished, and then etched lightly in Vilella's reagent. It is clearly seen in the two photomicrographs (Figures 5 and 6) that the cracks are quite straight with very little branching in evidence. A higher magnification photomicrograph (Figure 7) of the circled area "A" of Figure 5 gives the intimation of an intergranular crack which is further emphasized in the more etched structure in Figure 8. The crack in this photomicrograph appears to be intergranular (along prior austenite grain boundaries) in a basically tempered martensite matrix. Two other photomicrographs of the structure after full term etching (Figures 9 and 10) display the tempered martensitic structure which was common to both specimens.

SEM/EDS

The fracture face of disc #2 was examined by SEM/EDS. The low magnification fractograph (Figure 11) shows a "thumbnail-like" fracture, granular in appearance and covered with oxide scale. Three EDS scans were made across the fracture face (Figures 12 - 14a) prior to a deoxidizing treatment. The oxide film varied from crystalline to powdery in appearance. All of the scans had Fe and Cr present, while many of the scans had a Zn peak associated with them. One scan (Figure 12) also had Al and Si present. The appearance of Zn on the fracture face could not be explained, unless a Zn-based lubricant was used somewhere on the valve near the packing gland area. It appeared that the further the scan moved away from the initiation surface, the lower the Zn peak, until near the leading edge of the crack (Figures 14, 14a) no Zn was detected.

The fracture face was then deoxidized by the following treatment. A working solution of endox-214 was prepared by adding 8 ounces of endox-214 powder to 1000 ml of cold water and stirring until it was completely dissolved. A

small amount of photoflow was added to the solution to aid the wetting of the specimen and eliminate some of the featuring during the electrochemical cleaning step. A glass beaker with 500 ml of the endox-214 solution was placed in an ultrasonic cleaner. The specimen was made the cathode, and a platinum wire loop was used as an anode. A current density of 250 mA/cm^2 was applied for one minute. The specimen was removed from the electrolyte and ultrasonically washed in a detergent solution consisting of alconox and photoflow for another minute, then rinsed in clean water, dipped in methanol and dried in hot air. The above procedure comprises one cycle. It was occasionally necessary to repeat the above cycle several times before removing all the corrosion products. It was not possible to predetermine the exact number of cleaning cycles for any given specimen, since it depends upon the severity of the oxidation, roughness of surface, and the physical size of the sample. The specimen was observed optically after each cycle so that the process could be discontinued after the oxide or the corrosion product was removed and the specimen surface looks clean. After the specimen was thoroughly dried, it was examined immediately, since it may be prone to reoxidization at ambient atmosphere, or it was stored in a good desiccate.

The resultant fracture appearance after the deoxidizing treatment is displayed in Figure 15. It is clearly evident that the fracture is predominantly intergranular in appearance. Complete examination of the fracture disclosed no indication of fatigue interaction.

The fracture face of disc #6 was also examined (Figure 16) by SEM. The fracture face was also granular in appearance with no areas of fatigue interaction. Both EDS scans (Figures 17-18a) had Cr, Fe and Al associated with them. The scan furthest away from the initiation surface had no Zn associated with it, while the more heavily oxidized (darker) area near the initiation surface had both Zn and Si present in the scan.

The final fracture face examined was from disc #7 (Figure 19). The fracture was also granular and had a thumbnail appearance. EDS scans were performed across the fracture surface (Figures 20-22b). All of the scans had Cr, Fe, Zn and Al in common, with three of the four scans exhibiting a Si peak.

After examination by EDS the fracture face was deoxidized and examined by SEM. Figure 23 is a fractograph which shows the intergranular facets that were typical on this fracture.

Discussion/Conclusions

Type 410 stainless steel has been shown to be susceptible to stress corrosion cracking (SCC) in the presence of sulfides [1], chlorides [2], acids [3], and even in pure water environments [4].

In many cases, the cause of SCC can be attributed to the heat treatments received by the material prior to service introduction. The effect of heat treatment is so pronounced that the ASM Metals Handbook has a note specific to tempering of the 400 Series stainless steels [5], "....Tempering in the range of 700 to 1050F is not recommended, because it results in low and erratic impact properties and poor resistance to corrosion and stress corrosion."

In order to have stress corrosion cracking occur, three essential elements are required: a) tensile stress (either applied or residual), b) a susceptible microstructure, and c) a corrosive environment. If any of these is absent, SCC will not occur.

For the particular instance of the MSIV shaft at Farley Unit #1, the tensile stress could simply have been locked-in quenching stresses that had remained after the tempering operation. The susceptible material condition was tempered martensite which has been shown to be susceptible in pressurized water conditions [6] when tempered at too low a temperature. In fact, this same reference [6] recommended the use of AISI 410 stainless steel in pressurized water reactors only if it had been tempered above 1100°F. The Farley shaft was tempered at 950°F and used in a pressurized water reactor.

The failure analysis observations and the previously discussed literature references have led to the following conclusions:

1. The chemical analysis of the Farley Unit #1 MSIV shaft (#69C) showed that the chemical composition of the material was consistent with that expected of a Type 410 stainless steel.

2. The microstructure observed in the base metal (tempered martensite) is consistent with that expected in a Type 410 stainless steel in the quenched and tempered condition.

3. The hardness measurements (both R_c and Knoop) show that the hardness observed (R_c 41.3 with a KN max of 459) is significantly higher than that which was anticipated by the heat treatments performed.

4. The cracking was intergranular in nature, occuring along prior austenite grain boundaries.

5. There was no evidence of fatigue interaction on the fracture observed, and no definitive corrodent species identified.

6. The cracking is considered to be an intergranular stress corrosion cracking phenomenon resulting from a high hardness-susceptible material under pressurized water reactor conditions.

REFERENCES

1. Ishizawa, Y., Shimada, T. and Tanimura, M., Paper 124, Corrosion '82, NACE, March 22-26, 1982.

2. Lillys, P. and Nehrenberg, A. E., Transactions of the ASM, 48, pp. 327-345 (1956).

3. Bloom, F. K., Corrosion, 11, pp. 351t-361t, August 1955.

4. Trease, P. S. and McCartney, R. F., Corrosion, 16, pp. 26-30, March 1960.

5. Metals Handbook, 8th Edition, Vol. 2, p. 245, note d.

6. Suss, H., KAPL-2155, March 15, 1961.

TABLE 1

Chemical Analysis of Farley Unit #1 MSIV Shaft Sample

Element	Analysis (wt. %)	AISI 410 Requirements (wt. %)
Carbon	0.030	0.15 max.
Manganese	0.420	1.00 max.
Phosphorous	0.002	0.040 max.
Sulfur	0.015	0.030 max.
Silicon	0.350	1.00 max.
Chromium	11.800	11.50 - 13.50
Nickel	0.250	-
Molybdenum	0.030	-

TABLE 2

Hardness Measurements of Farley Unit #1 MSIV Shaft Sample

Microhardness Measurements (KN/500 gms)

439	445
424	452
431	445
445	459
452	445

Average - KN 444
Equates to R_C 43.4

Rockwell Hardness Measurements (C-Scale)

41.0	41.0
41.5	41.5

Average - R_C 41.25

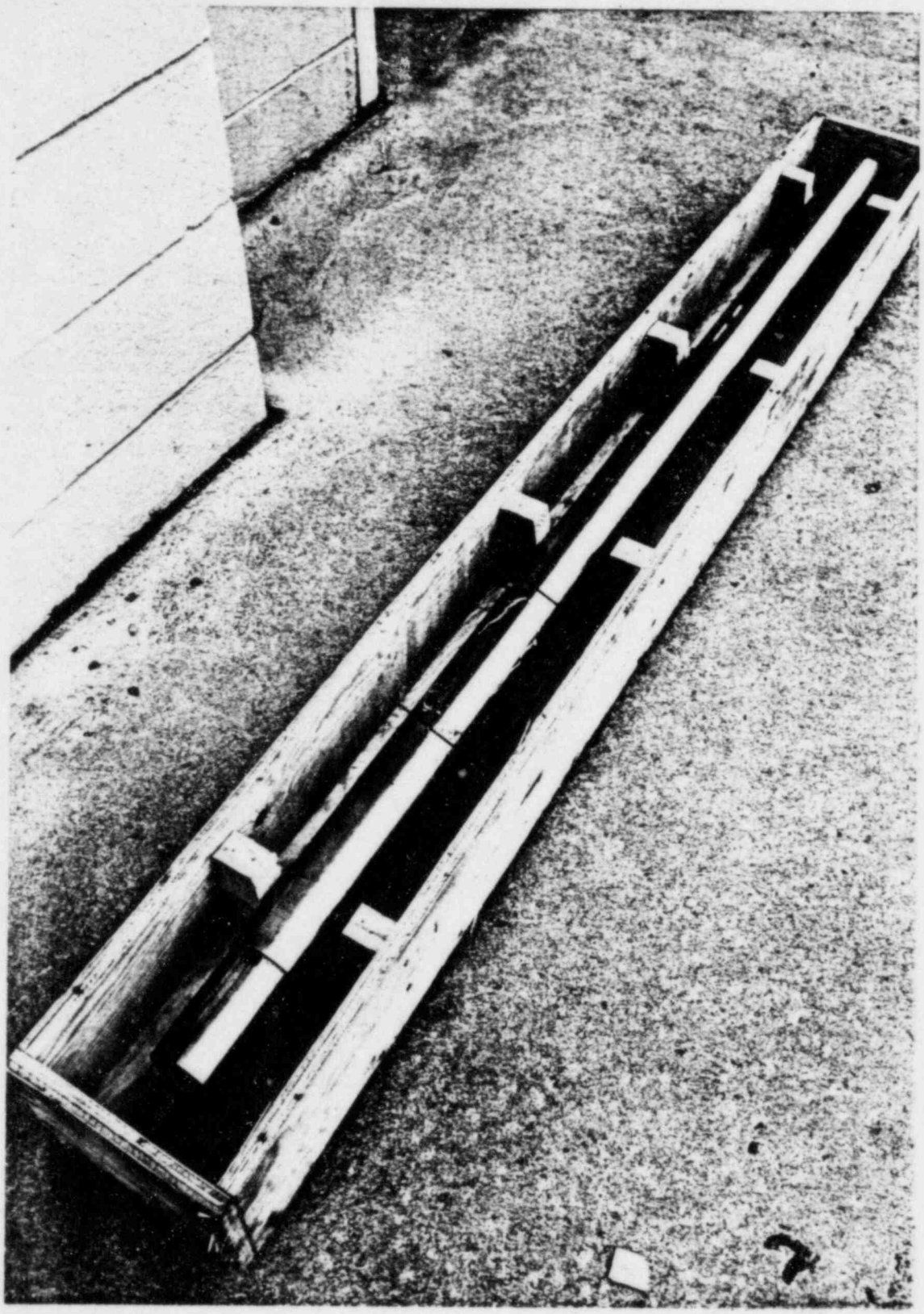

FIGURE 1. Photograph of 77" MSIV shaft from Joseph M. Farley Unit #1. Outlined area is location of cracking.

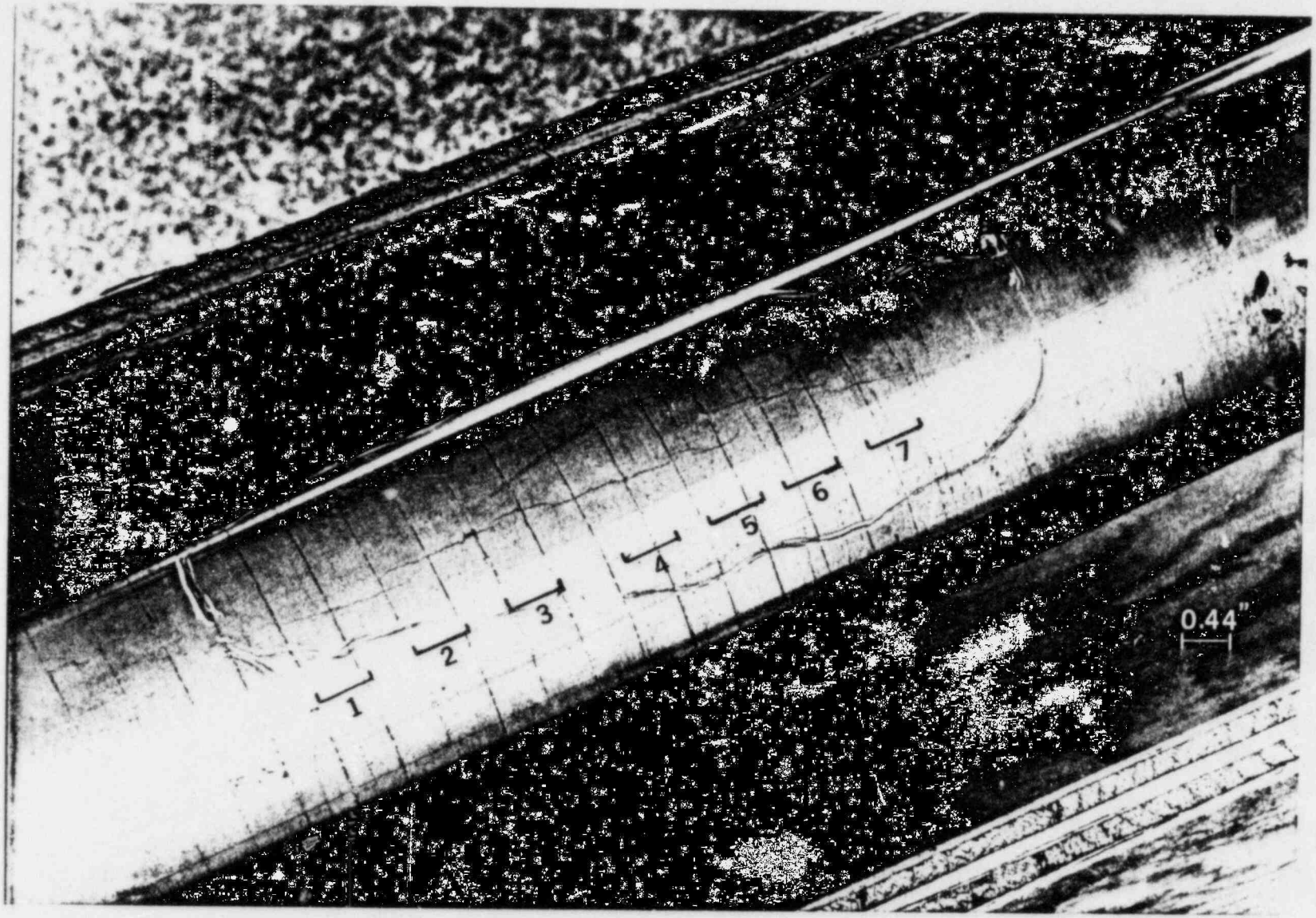

FIGURE 2. Photograph of cracks on MSIV shaft. Numbered areas are approximate locations of specimen cuts.

FIGURE 3. Photograph of the fracture face of Specimen #2 showing thumbnail characteristics and darkened area (between the arrows) near the crack initiation surface.

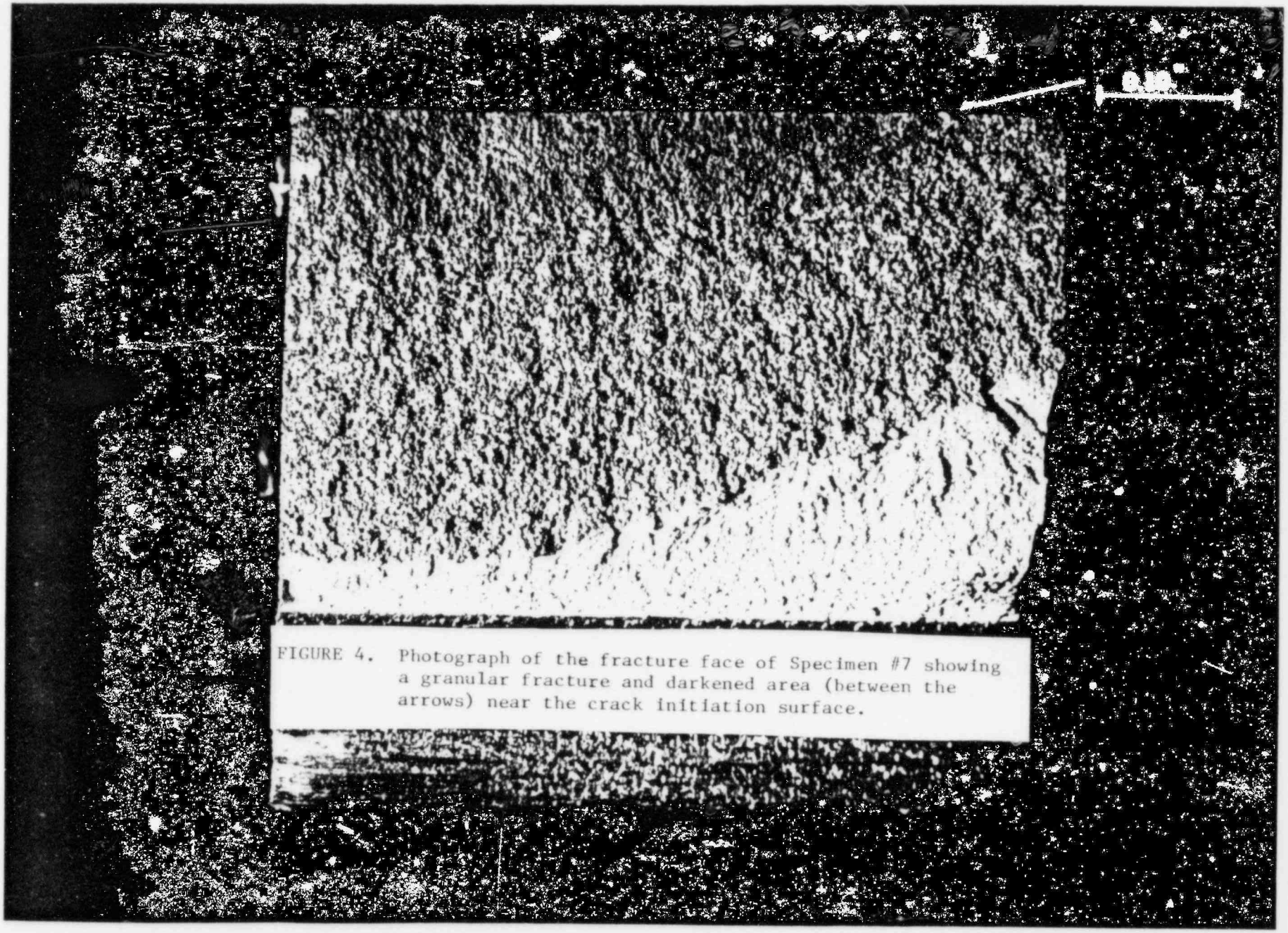

FIGURE 4. Photograph of the fracture face of Specimen #7 showing a granular fracture and darkened area (between the arrows) near the crack initiation surface.

FIGURE 5. Low magnification photomicrograph of the cracks on Specimen #4 from the Farley MSIV.

FIGURE 6. Low magnification photomicrograph of the cracks in evidence on Specimen #5 from the Farley MSIV.

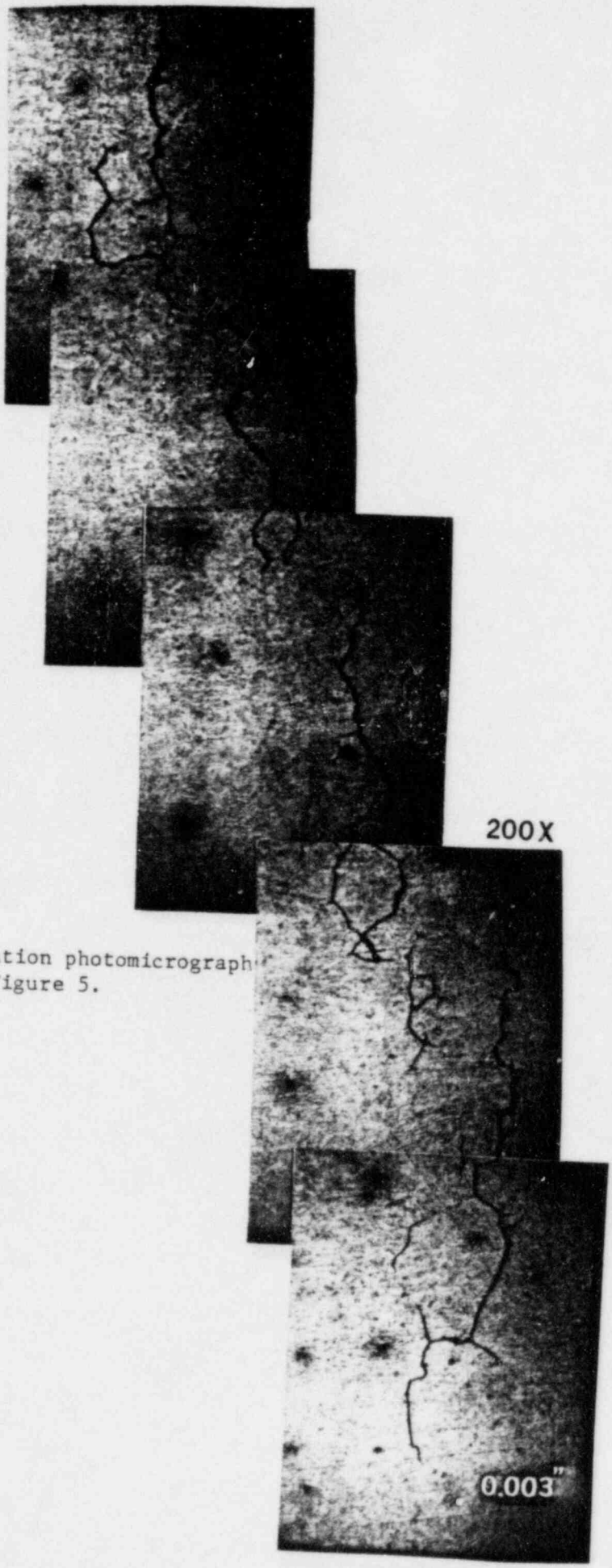

FIGURE 7. Higher magnification photomicrograph of Area "A" in Figure 5.

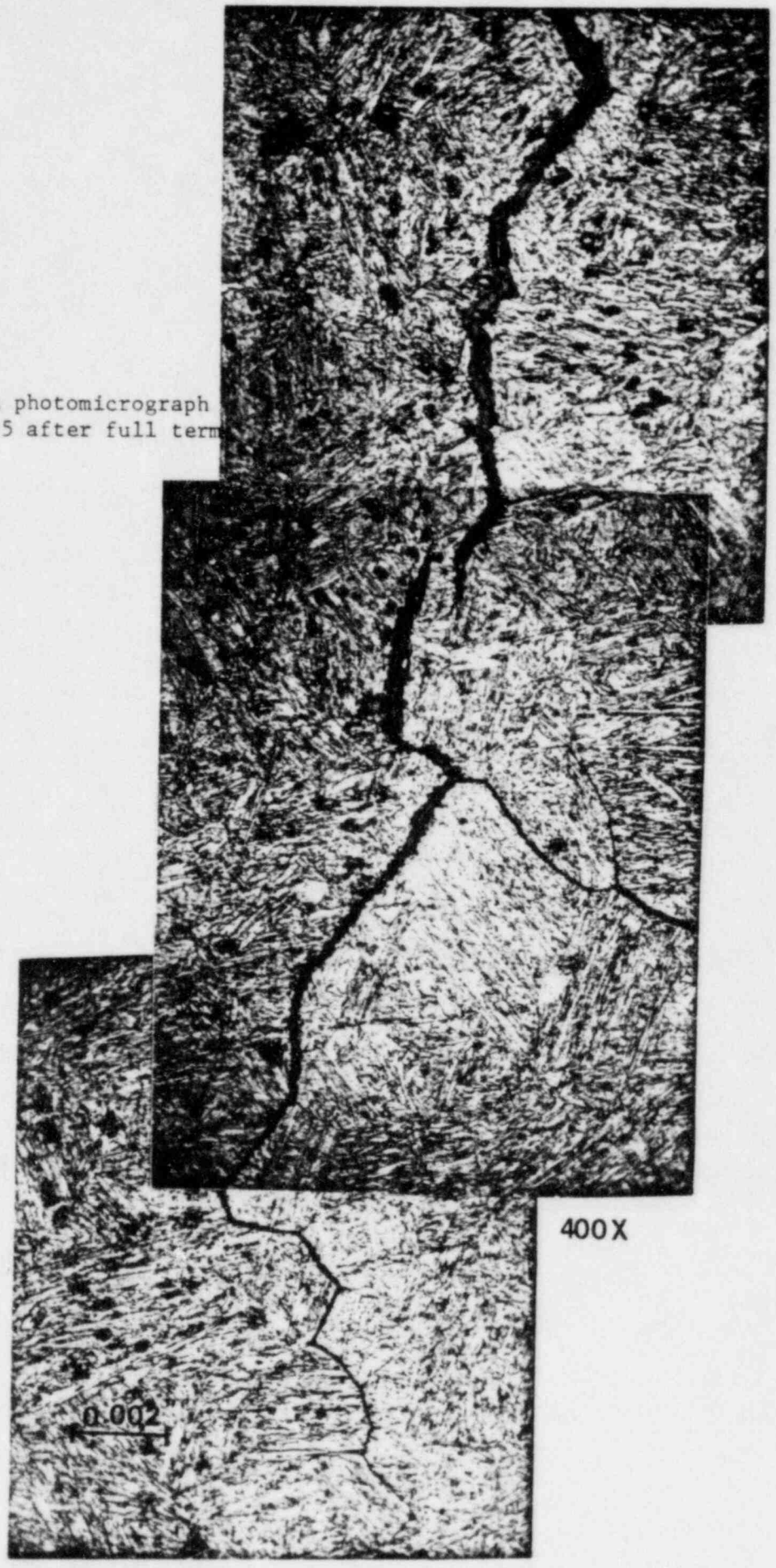

FIGURE 8. High magnification photomicrograph of crack on disc #5 after full term etching.

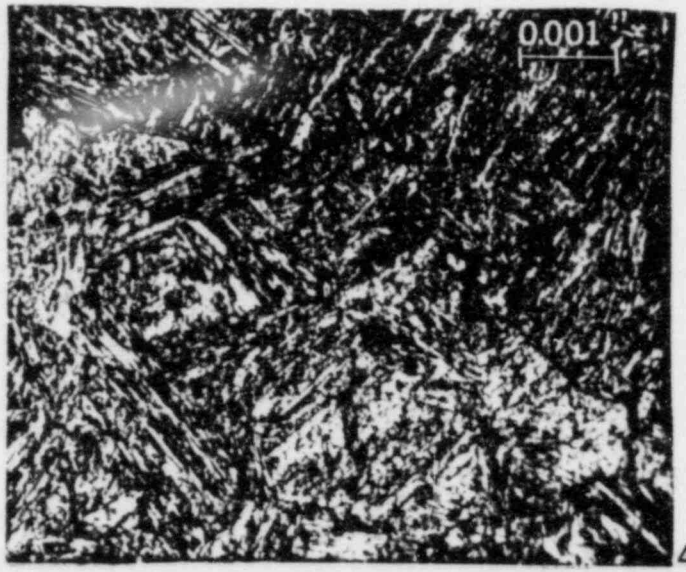

FIGURE 9. Photomicrograph showing structure of disc #4 as tempered martensite.

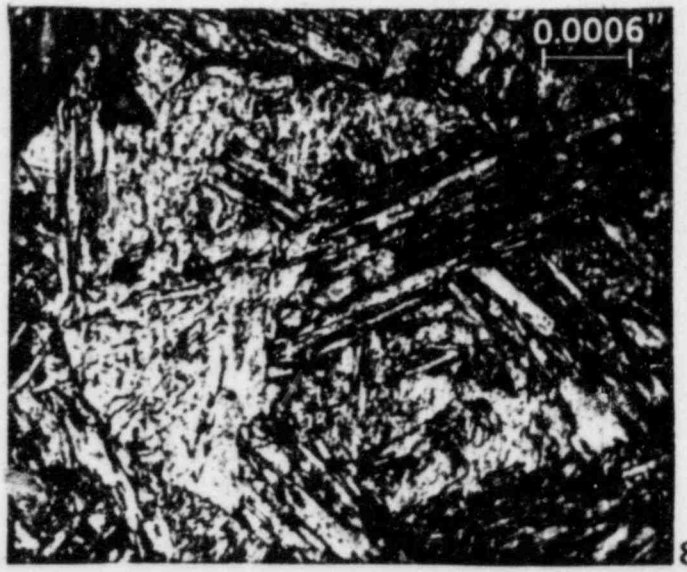

FIGURE 10. High magnification photomicrograph of disc #5 showing structure.

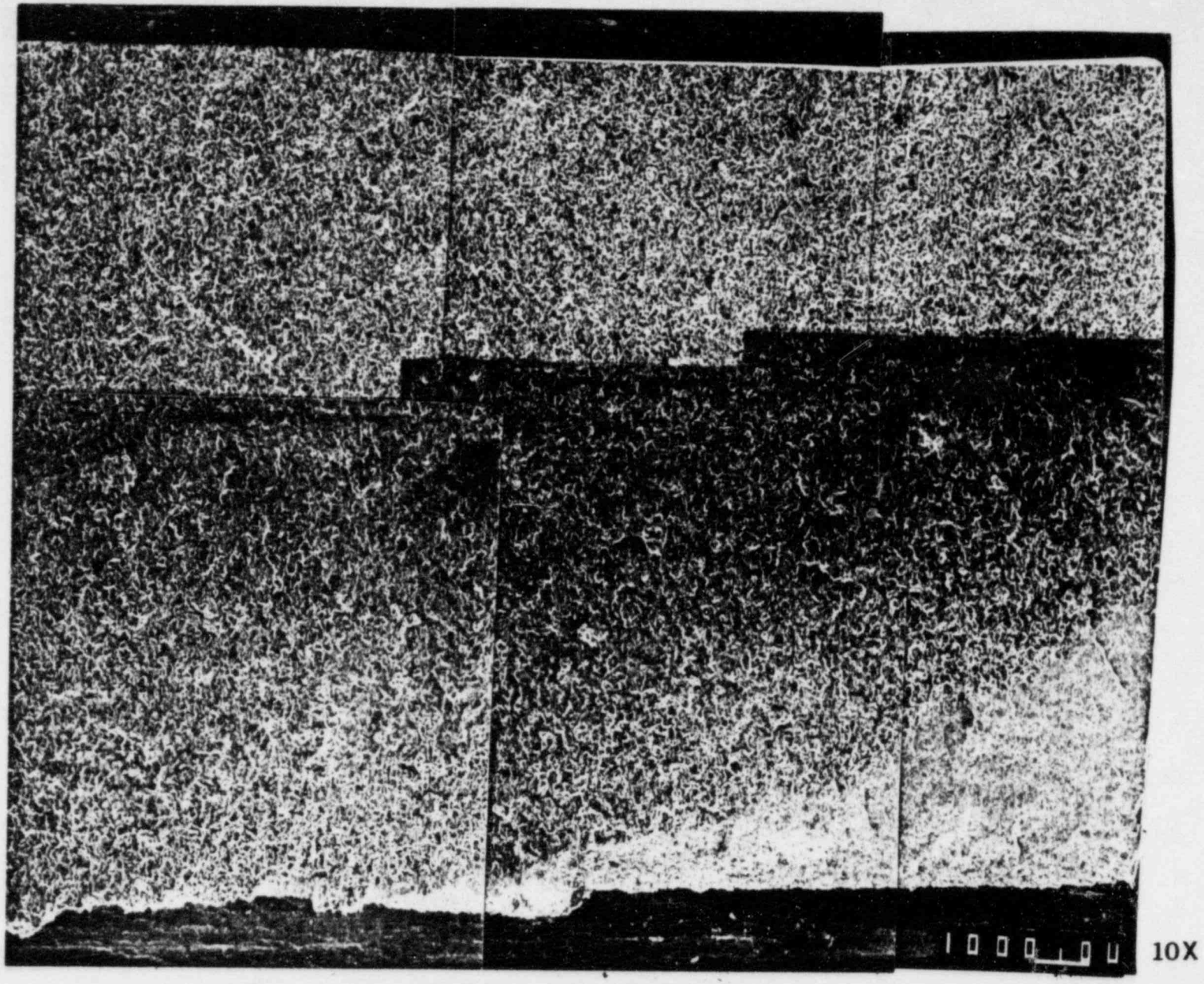

FIGURE 11. Low magnification fractograph of disc #2 fracture face showing granular appearance.

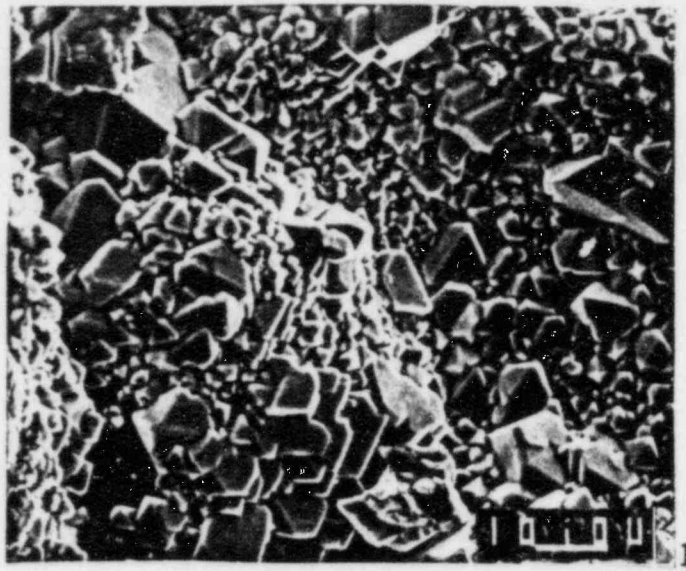

FIGURE 12. Fractograph of dark oxide area of disc #2.

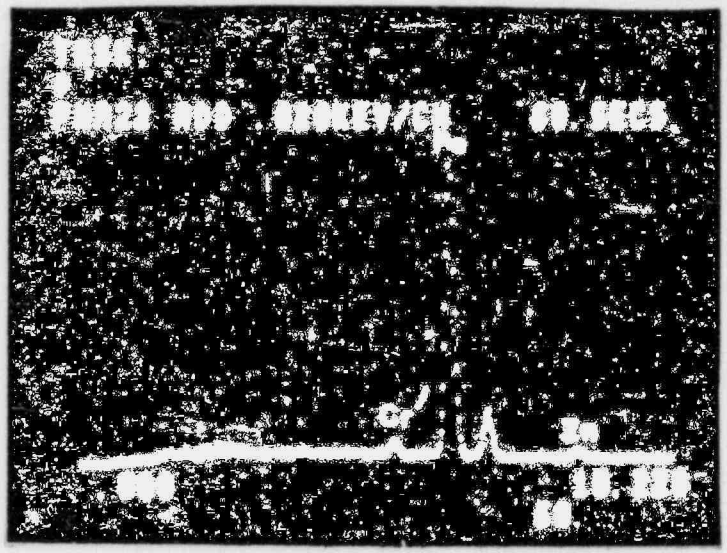

FIGURE 12a. EDS scan of dark oxide area for constituents.

FIGURE 13. Powder like oxide is seen on the second fractograph of disc #2.

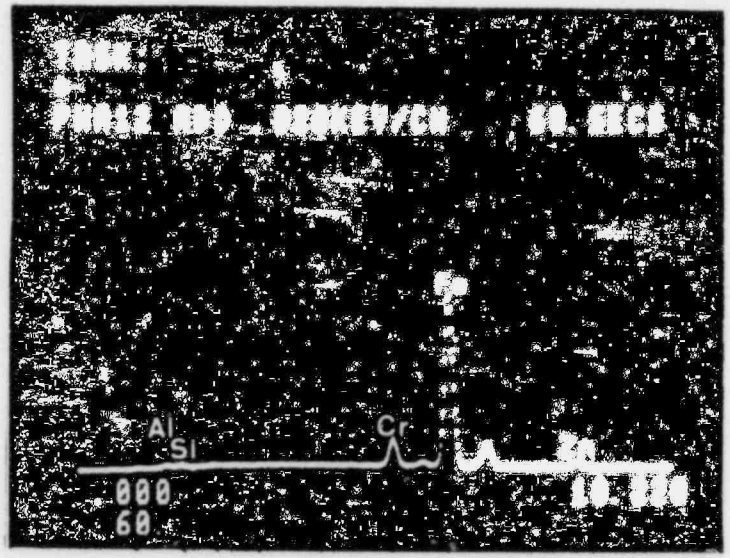

FIGURE 13a. Chemical analysis of oxide by EDS.

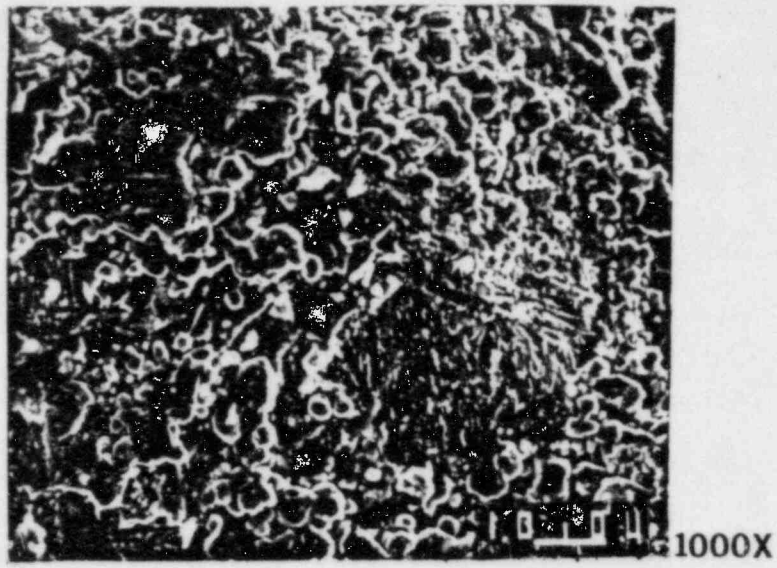

FIGURE 14. SEM photo of third scan on disc #2 -- farthest scan away from initiation surface.

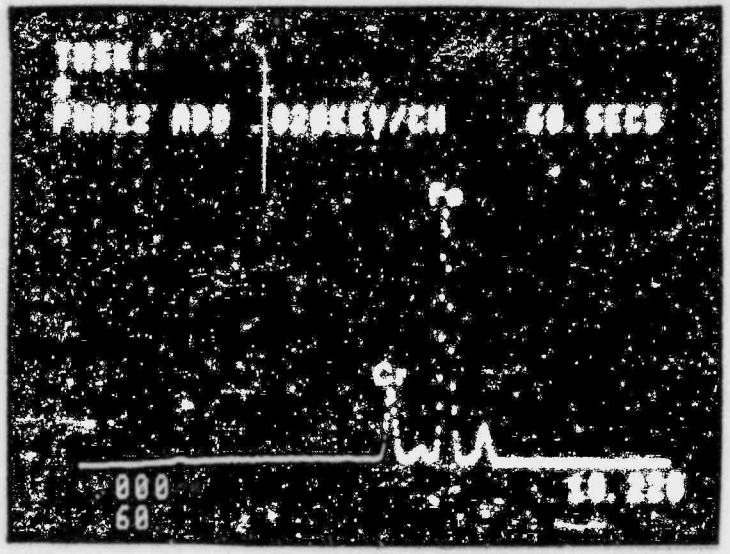

FIGURE 14a. EDS scan of area for constituents -- note the absence of Zn.

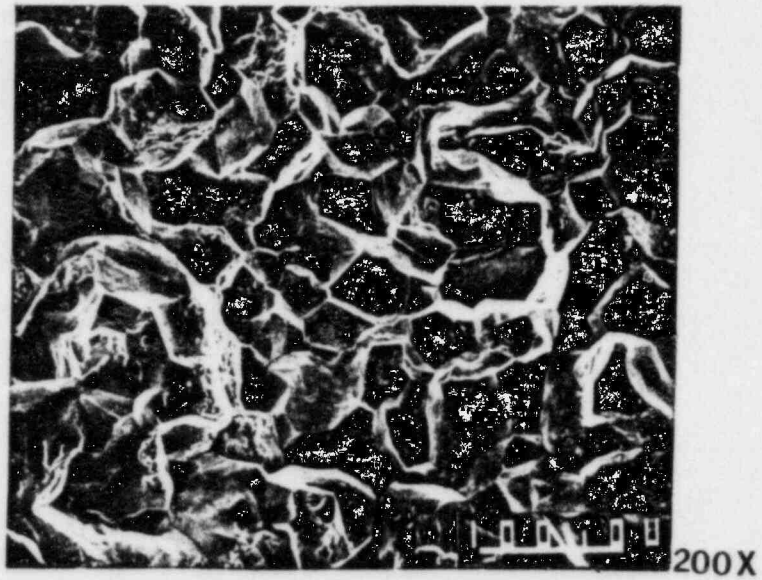

FIGURE 15. Intergranular structure of disc #2 fracture surface is evident after deoxidizing treatment.

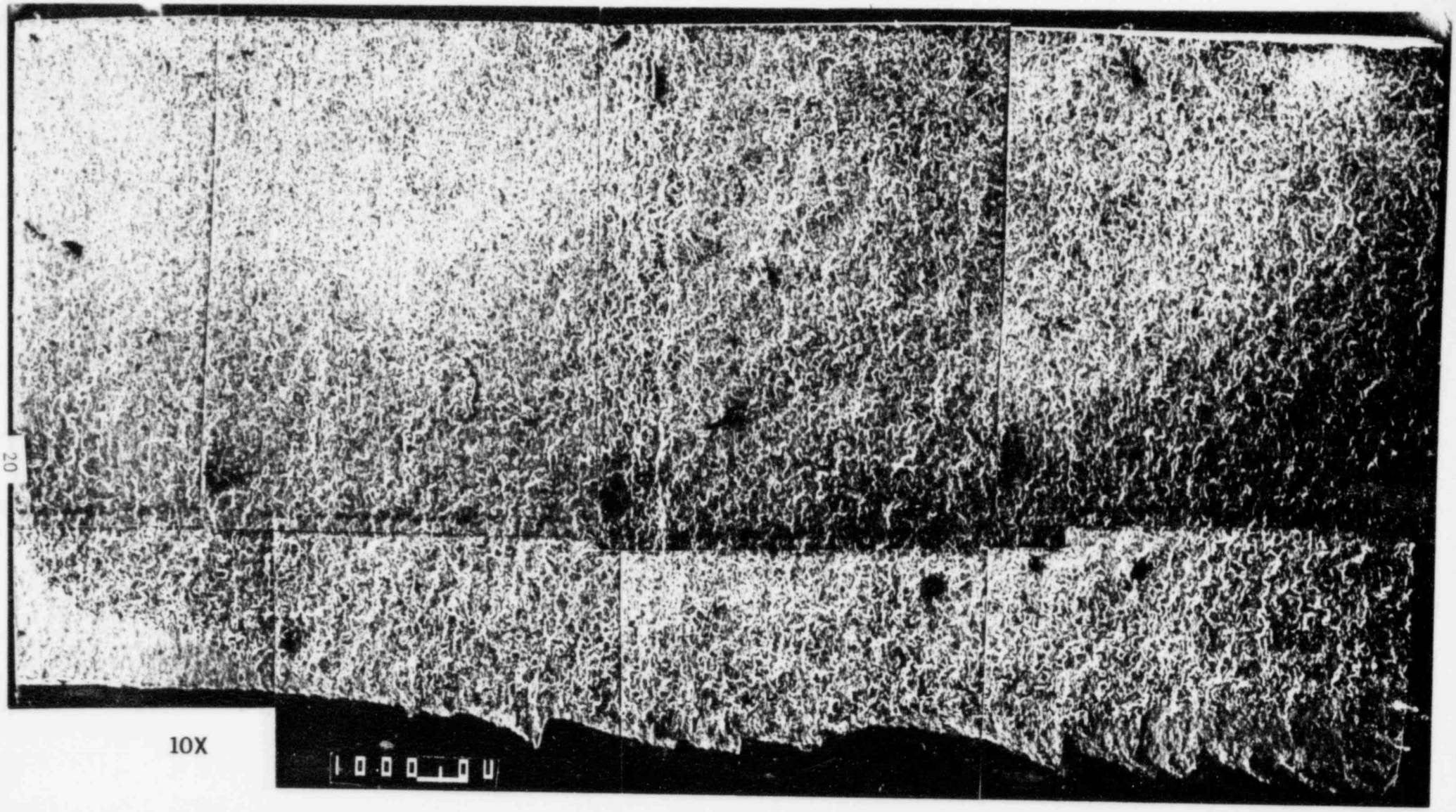

FIGURE 16. Low magnification SEM photo of the fracture on disc #6.

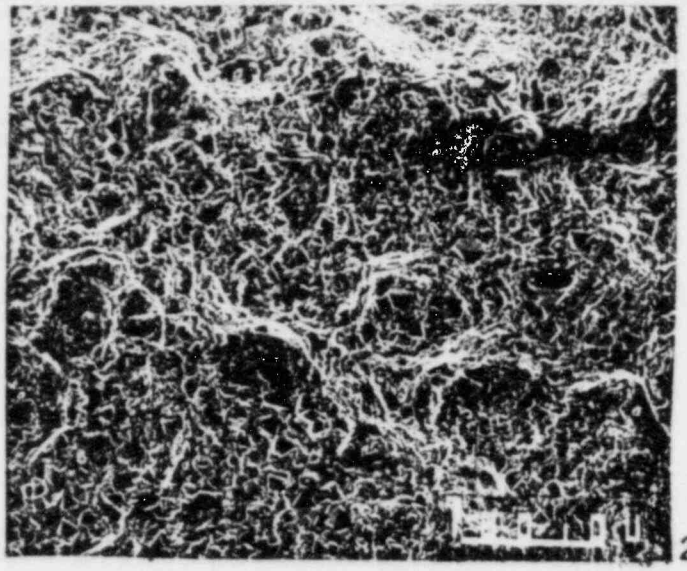

FIGURE 17. SEM photo of fracture face from disc #6 — farthest from initiation surface.

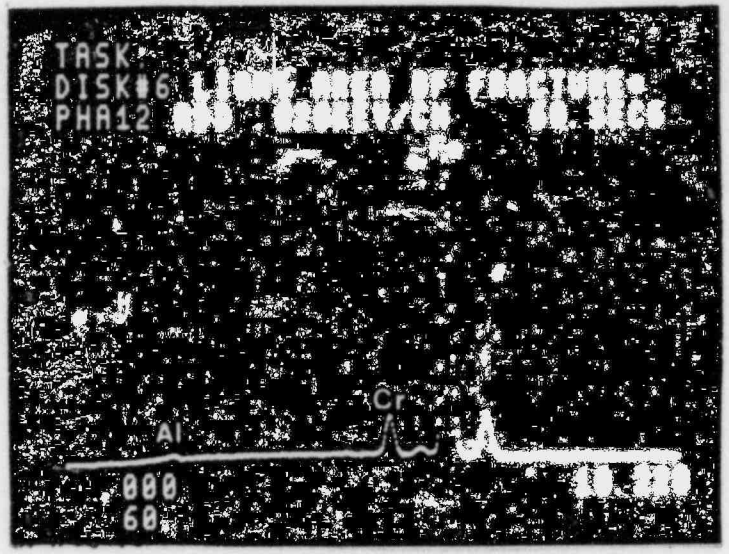

FIGURE 17a. EDS scan of area for constituents -- note the absence of Zn.

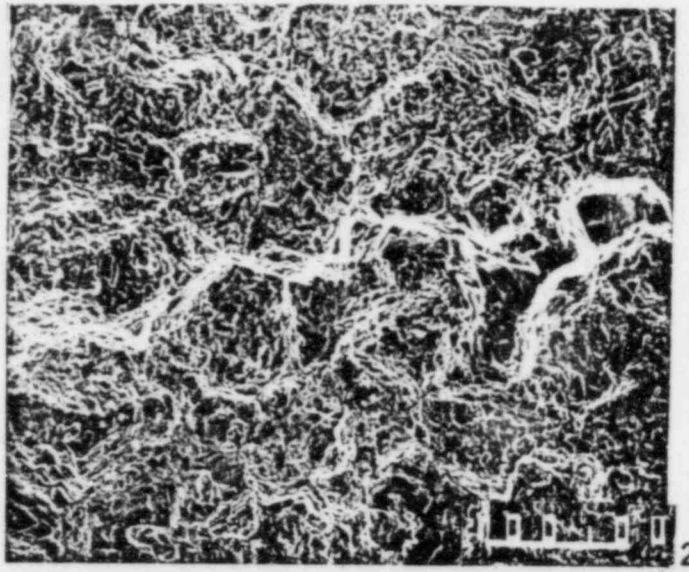

FIGURE 18. Fractograph of dark oxide area of disc #6.

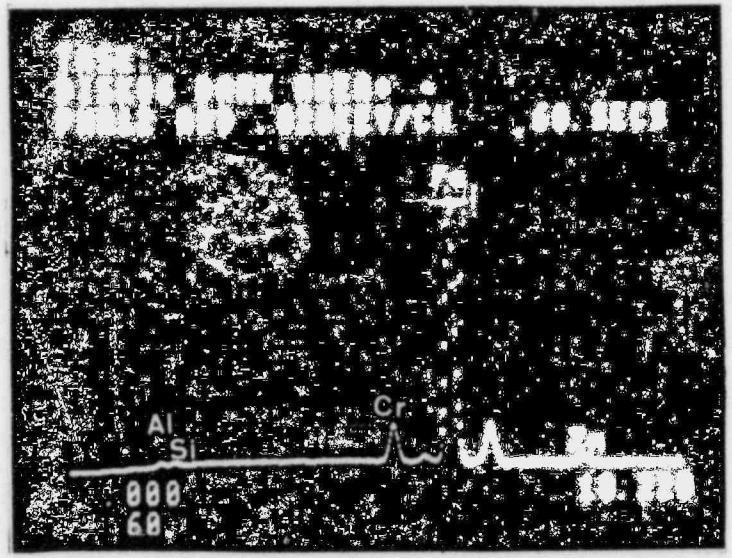

FIGURE 18a. Chemical analysis of constituents in fracture area.

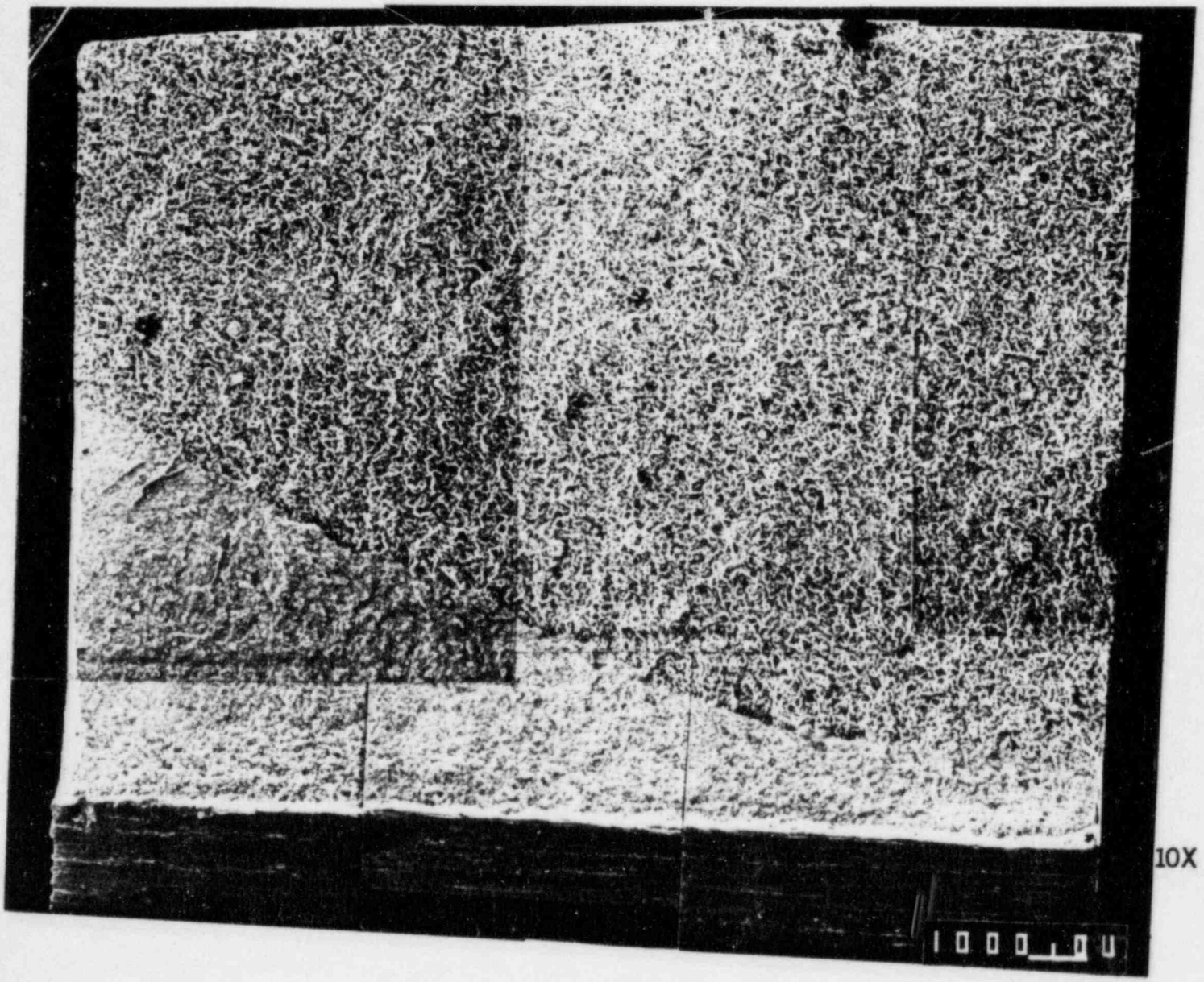

FIGURE 19. Low magnification fractography of the fracture face from disc #7.

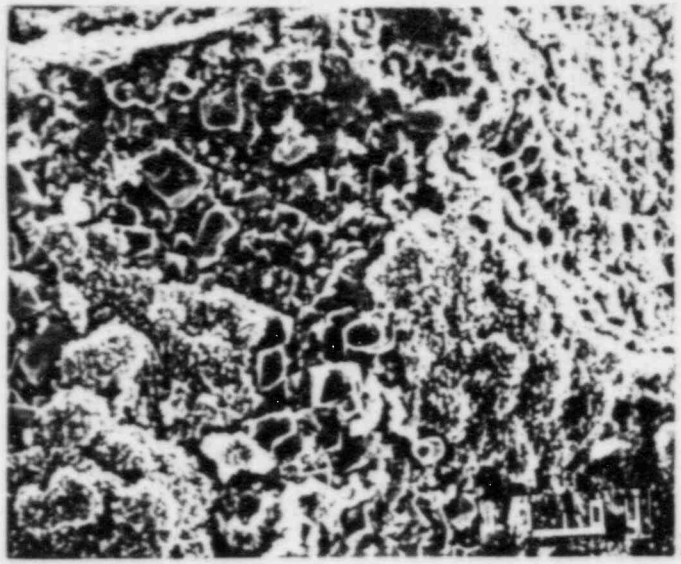

FIGURE 20. SEM photo of disc #7 near initiation surface.

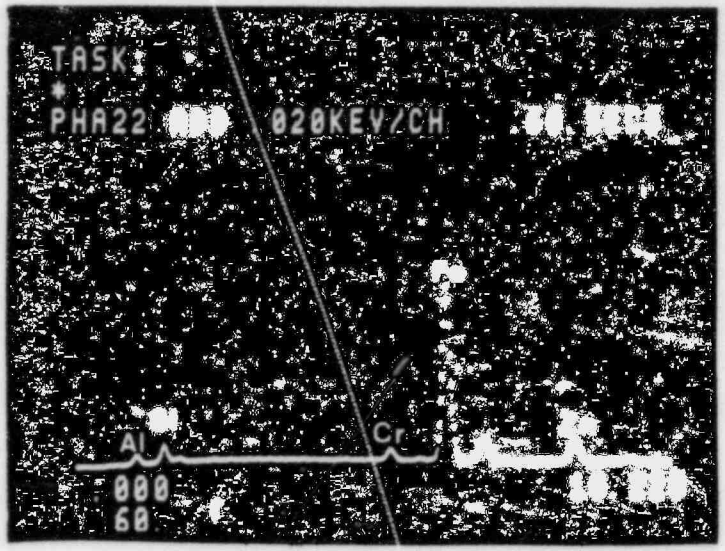

FIGURE 20a. EDS scan of area for constituents.

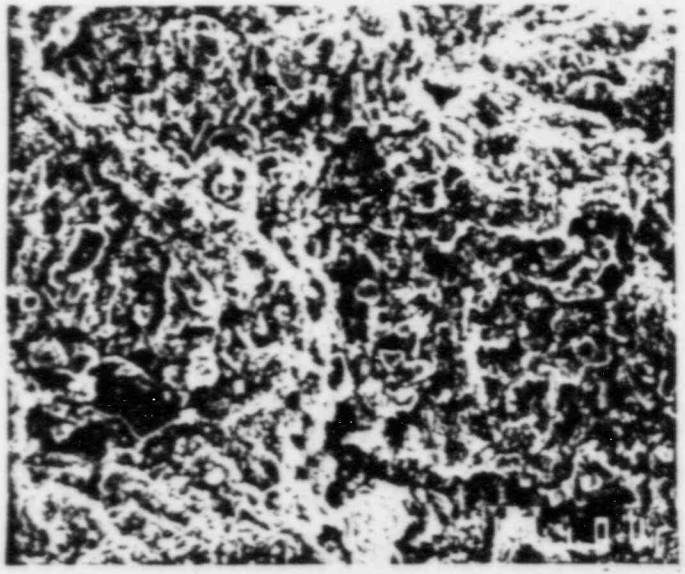

FIGURE 21. Fractograph of area on disc #7 -- farthest away from initiation surface.

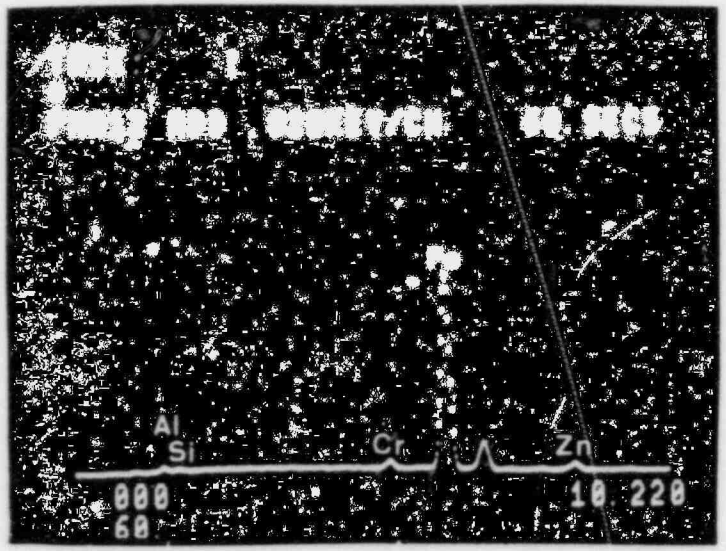

FIGURE 21a. Chemical analysis of area by EDS.

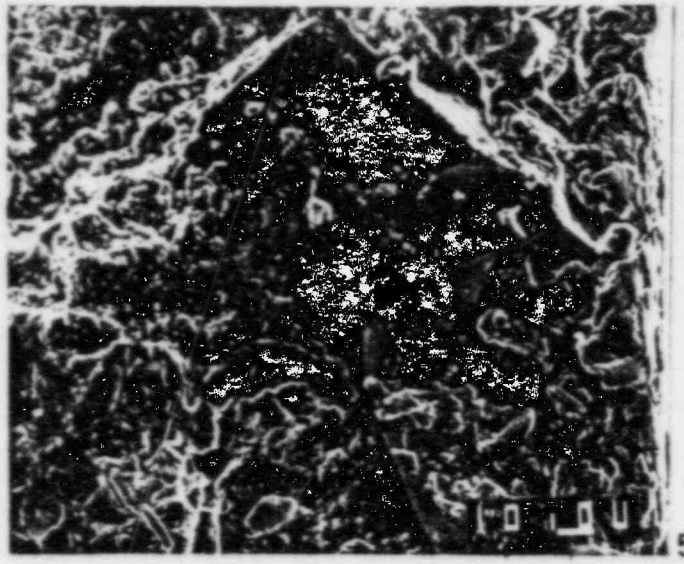

FIGURE 22. SEM photo of an intergranular facet on disc #7.

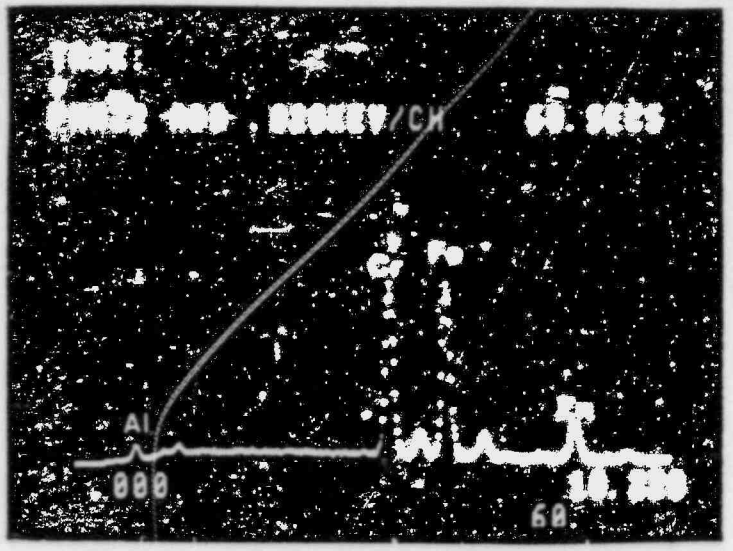

FIGURE 22a. EDS scan of area to the lower left of the facet.

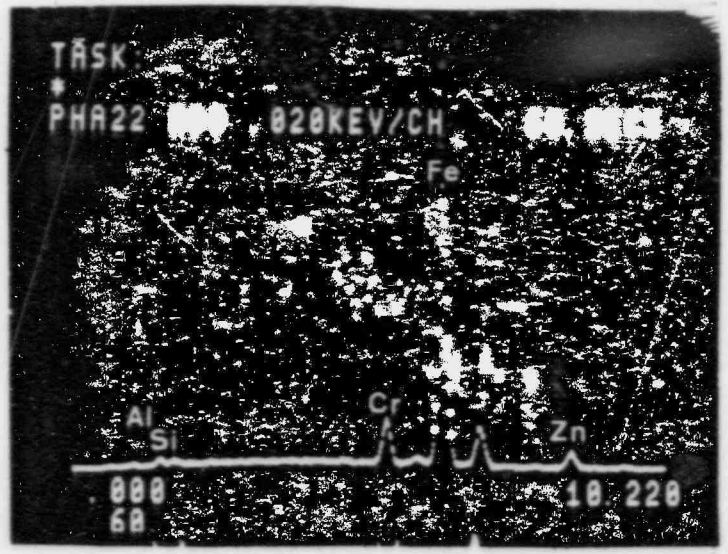

FIGURE 22b. EDS scan of intergranular facet's surface.

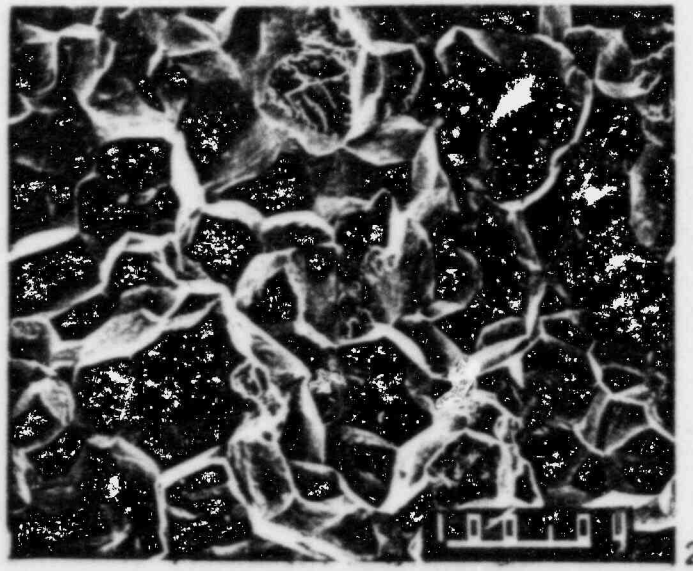

FIGURE 23. Fractograph of intergranular nature of disc #7 fracture after deoxidizing treatment.

APPENDIX B

INVESTIGATION OF A FEEDWATER REDUCER FROM FARLEY UNIT 1